Scalable graphene production from ethanol decomposition by microwave argon plasma torch

C. Melero[1], R. Rincón[1], J. Muñoz[1], G. Zhang[2], S. Sun[2], A. Perez[3], O. Royuela[3], C. González-Gago[1] and M.D. Calzada[1]*

[1] Laboratorio de Innovación en Plasmas (LIPs), Edificio Einstein (C2), Campus de Rabanales, Universidad de Córdoba, 14071 Córdoba (Spain)
[2] Institut National de la Recherche Scientifique (INRS), Énergie, Matériaux et Télécommunications, 1650 Boulevard Lionel-Boulet, Varennes, QC J3X 1S2, Canada
[3] Iberfluid Instruments S.A. C/ Botánica 122, 08908 Hospitalet de Llobregat (Barcelona, Spain)

Abstract

A fast, efficient and simple method is presented for the production of high-quality graphene on a large scale by using an atmospheric-pressure plasma-based technique. This technique allows to obtain high quality graphene in powder in just one step, without the use of neither metal catalysts and nor specific substrate during the process. Moreover, the cost for graphene production is significantly reduced since the ethanol used as carbon source can be obtained from the fermentation of agricultural industries. The process provides an additional benefit contributing to the revalorization of waste in the production of a high-value added product like graphene. Thus, this work demonstrates the features of plasma technology as a low cost, efficient, clean and environmentally friendly route for production of high-quality graphene.

E-mail: md.calzada@uco.es (Maria Dolores Calzada)

Keywords: graphene, plasma, microwave, TIAGO, ethanol, catalyst-free

1. Introduction

Graphene is a two-dimensional carbon material (2D material) which can be considered as the basic structure of all known graphitic materials such as fullerenes, carbon nanotubes (CNTs) and graphite. During the last years, the interest of the scientific community in the graphene has increased considerably due to its wide range of applications in fields such as electronic, catalysis, energy storage and composite materials; applications that are based on the novel electrical and mechanical properties of this material [1-6]. Thus, the development of synthesis processes with posibilities to be scalable at industrial level is one of the main objectives of research laboratories and companies.

Although high quality graphene can be obtained from highly oriented pyrolytic graphite (HOPG) by mechanical exfoliation [7,8] anodic bonding [9,10] or laser ablation [11,12], the use of these techniques does not allow to scale up its production for commercial applications. *Chemical Vapour Deposition* (CVD) and *Liquid Phase Exfoliation* (LPE) are scalable techniques widely used for the graphene production. However, its use presents some limitations. In the case of CVD, graphene is always supported on a specific substrate, being Ni and Cu the most used metals as catalysts. Then, its quality depends on the nature of the substrate limiting its use in certain applications. Besides the need of catalyst, the addition of an excess of hydrogen is necessary to activate the catalysis [13-15] and high temperatures are also required, which implies a high economic cost. LPE is a substrate-free graphene synthesis method with a relatively low production costs [16-18]. This technique consists in the dispersion of graphite in an aqueous or non-aqueous solvent followed by exfoliation by using, for instance, ultrasounds. The material produced by LPE uses to present a large number of defects, probably due to the exfoliation itself and/or the purification processes used for removing the un-exfoliated graphite flakes~~.~~ but a scalable method for producing large quantities of graphene defect free by LPE has been reported during the last years [19]. However, the obtained graphene is suspended in a solvent~~s, then~~ restricting its application~~ed~~. Then, ~~these two~~ the available scalable techniques, CVD and LPE, do not allow to obtain high quality graphene powder in one step, needing complementary treatments to extract it from the substrate (CVD) or the solvent (LPE), reducing the technological fields in which can be applied.

During the last years, plasma, defined as a partially ionized gas, mainly composed by electrons, ions, neutral atoms and photons, has emerged as a promising technology, complementary/alternative to conventional methods, for the production of nanostructured carbon material by using different precursors as carbon source [20-22] being the energy of the plasma particles (~ 500 K) enough for decomposing organic molecules into their atomic elements, that can later recombine at the plasma exit forming compounds different to those initially introduced.

Plasma Enhanced Chemical Vapor Deposition (PECVD) was the first plasma-based technique applied to the synthesis of graphene [23–30]. PECVD can significantly reduce the graphene production costs because it works at lower temperatures than the conventional CVD process; however, PECVD shows some of the limitations ~~as~~ of CVD technique (substrate and low pressure requirements).

Recently, microwave plasmas have been reported as efficient, clean and enviromentally friendly tool for the synthesis of calatlyst-free graphene by using ethanol as carbon source [20-22] which is of special interest since a surplus can be derived from the biomass via fermentation then allowing the revalorization of waste for producing a high-value added product like graphene. Microwave plasmas can operate at relatively low powers (< 1 kW), presenting high stability and reproducibility within a wide range of operational conditions. Furthermore, the possibility of working at atmospheric pressure, make them an economic and attractive technique for implementation of the process at industrial scale, reducing the production costs. Atmopsheric-pressure microwave plasmas are non-thermal plasmas in which the average energy of electrons and heavy particles (above 7000-10000 and 1200-3000 K, respectively) are larger than those required for decomposing organic compounds. Due to the difference in temperature (energy) between electrons and heavy particles, lower energies are required for creating and maintaining these discharges. Then, more energy is available to induce physical and chemical reactions for the generation of radicals and excited species into the plasma [31,32]. Besides, in atmospheric-pressure plasmas the great number of electrons colliding with the plasma heavy particles avoids the recombination of species into large chain molecules at the plasma exit limiting the size of the by-products [33].

Dato's group [21,34] in 2008 and later Tatarova's group [22,35] in 2013 were the first groups that reported the synthesis of high quality graphene from ethanol by using atmospheric pressure microwave plasmas. Dato [21] reported the use of 84 mg of ethanol per each mg of graphene obtained. No details about graphene production were reported in Tatarova's work. Both processes produce high-quality graphene with relatively low ethanol costs being the synthesized graphene collected in a nylon filter. Therefore, its extraction requires of a subsequent treatment by using a solvent. In 2015, Rincón *et al.* [20] proposed a procedure by which a mixture graphene/carbon nanotubes was obtained in an amount of 4 mg/h, but the graphene percentage contained in this mixture was not reported. In summary, the processes described in these papers show the possibility of producing graphene but they do not solve one of the most important challenges faced by the scientific community, i.e., the direct production of graphene powder for scale up production.

In this paper, we report high-quality graphene production by a special microwave plasma torch using ethanol as carbon source and Ar as carrier gas. The plasma is generated

by a TIAGO device developed by Moisan's group [36]. A detailed theoretical and experimental description was reported in [37,38]. The proposed synthesis process is carried out by a single step and no metal catalyst is needed. Graphene powder is directly obtained from the ethanol decomposition and extracted from a reactor designed for this purpose without any further treatment in contrast to other procedures in wich the graphene is gathered on a nylon membrane [21,22] or a filter [20] placed after the plasma.

The advantage of the TIAGO device in comparison with those used by Dato [21,34], Tatarova [22,35] and Rincón [20] are the following ones:

a) TIAGO torch has higher tolerance to ethanol injection and large power densities are delivered to the discharge compared to other field applicators such as resonant cavities or waveguides [39,40] and other microwave devices [20,41]; besides, the high values of electron density and temperature of this torch also favor the decomposition of substances and their excitation [20,41],

b) it does not present the contraction and filamentation phenomena tipycally observed in microwave plasmas generated in dielectric tubes at atmospheric pressure. Nevertheless, these phenomena, depending on the thermal conductivity of the plasma gas and the discharge tube diameter [42],-can be avoided by using discharge tubes of small internal radius [43] or vortex configuration [44,45], and

c) as it can be read in [36] "*it is possible to arrange TIAGOs in arrays to form a compact torch system which can be supplied with equal distribution of power between plasma flames from a single waveguide, that is, the TIAGOs arrays can be operated at 2.45 GHz with powers of a few hundred watts up to 2-3 kW per nozzle. This unique feature makes this device particularly suitable to be implemented at industrial level*".

In this context, with the current research we contribute to present the microwave plasma TIAGO torch as an economic and attractive technique for the implementation of the graphene synthesis at industrial scale, reducing the production costs.

2. Experimental set-up and analysis methods of carbon material

2.1 Plasma system

Figure 1a shows a picture of the TIAGO torch. This specific device is constituted by a waveguide whose central section is reduced in height and a cylindrical hollow metallic rod placed perpendicularly to it. The plasma gas flows inside the rod to the tip, where the plasma is created and the discharge can be considered as a jet conical flame surrounded by the air around it. In order to use this device in the ethanol decomposition, the TIAGO device was modified by adding a glass reactor coaxially placed around the metallic rod (Figure 1b). Reactor consits in a glass cylinder manufactured with three outflows which can be maintained opened or closed as it is described in our previously published works

[37,38,46]. Besides, a quartz window was added to the reactor in order to register the radiation emitted by the discharge avoiding the UV-region radiation absorption. In the current research, the outflow placed at the top was opened to evacuate the gases formed from the ethanol decomposition and, therefore, maintaining atmospheric pressure into the reactor. The ouflow placed in the lower part of the reactor was closed after switching the plasma on and the other one was coupled to a mass spectrometer to monitor the nitrogen content coming from the surrounding air into the reactor. Ethanol was introduced into the plasma once the nitrogen amount was constant.

In the current research, the glass reactor plays two significant roles. First, it reduces the contact of the plasma with the atmospheric air and, consequently, avoids the instabilities produced by the air stream. The influence of the surrounding air on the plasma has been studied in previous works, and the results shown that the air entrance into the plasma not only modifies the equilibrium properties and discharge kinetics of the Ar plasmas [37,38], but also induces changes in the decomposition routes of ethanol [46,47]. This air entrance provokes a decrease of the gas temperature, reducing the energy of the plasma heavy particles and it modifies the reaction kinetics in which these particles take part. Besides, the presence of air components (N_2 and O_2) in TIAGO plasmas favours the formation of CN species due to the interaction of nitrogen with carbon atoms coming from the ethanol decomposition. Formation of CN prevents the formation of C_2 radicals that are the precursor species of the graphene material. As it was reported elsewhere [48,49], the presence of an oxidizing component (oxygen or water) in the plasma hinders the production of solid carbon, favouring the formation of both CO_2 and CO at the plasma exit.

Furthermore, the reactor is used as a chamber to retain the solid species resulting from the ethanol decomposition. In our case, the plasma flame occupies the reactor center and the carbon species generated in the discharge are deposited in the inner walls of reactor. Therefore, they can be directly collected without needing the use of solvent and complementary processes.

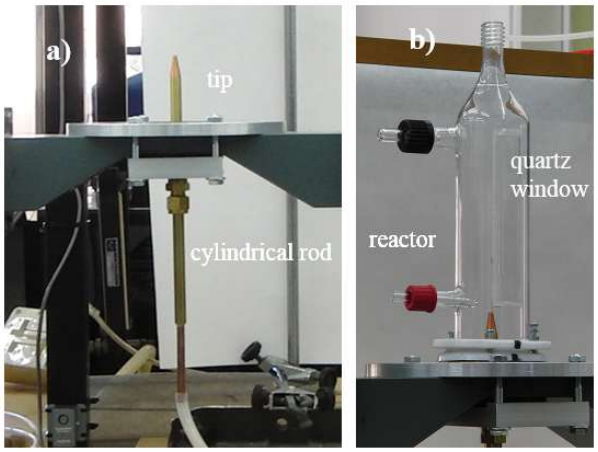

Figure 1. a) TIAGO torch and b) Reactor.

Microwave power (300 W) was supplied to create and maintain the discharge in continuous mode by a 2.45 GHz SAIREM microwave generator (GMP kG/D) equipped with water cooled circulator to avoid power reflection damage. A short circuit movable plunger and a triple stub was used to match the impedance and stabilize the plasma keeping the reflected power below 5% of the input power [37,38].

High purity (99.999%) argon gas was used to initiate and feed the discharge using Bronkhorst Mass Flow Controller. An Ar flow of 1 L/min was used in this research since the formation of solid carbon from the ethanol decomposition is favoured from this flow [46,47]. In previous studies [46], we demonstrated that the use of ethanol concentrations larger than 2% resulted in flame extinction. Therefore, we chose 2 g/h of ethanol which corresponds 2% (V/V) of ethanol in the argon-ethanol (Ar-EtOH) mixture. Ethanol was vaporized by a Controlled Evaporator Mixer (CEM, Bronkhorst) before being introduced into the plasma. The CEM-System (Controlled Evaporation and Mixing) is an innovative Liquid Delivery System (LDS) that can be applied for atmospheric or vacuum processes. The vapour generation system consists of a Coriolis liquid flow controller (LIQUID-Flow®) for ethanol, a Mass Flow Controller (EL-FLOW®) for Ar which acts as carrier gas and a temperature controlled mixing/evaporation device. The components forming part of the CEM-system were integrated in a single panel designed by Iberfluid Instruments S.A. (Figure 2). Ethanol was placed in a small tank pressurized with helium to ensure proper working of the liquid flow controller. This vaporization system can replace bubblers with better performance, stability and accuracy [50]. Once Ar plasma was ignited Ar-EtOH gas mixture was added to the TIAGO plasma through a steel tube heated at 110 °C to prevent ethanol condensation.

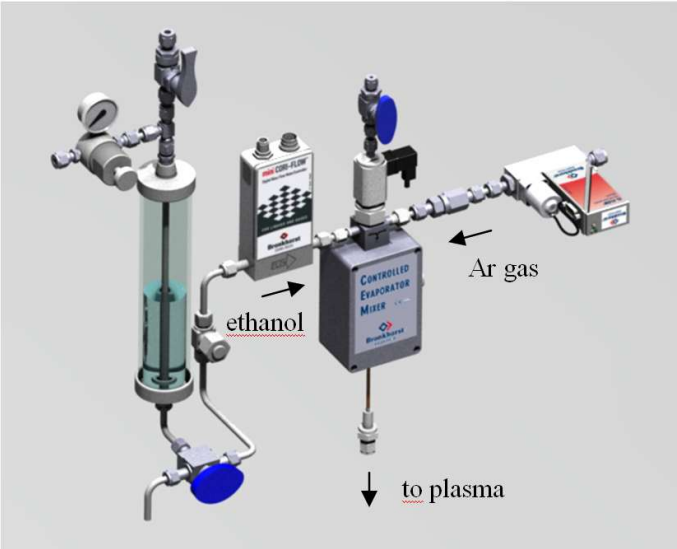

Figure 2. CEM-system utilized for the vaporization of ethanol before its entrance into the plasma.

2. 2 Analysis techniques

The plasma capability of inducing the decomposition of ethanol molecules and the species formed was analysed from the radiation emitted by the plasma. This radiation was collected at a height of 0.5 mm above the tip of the torch and directed by an optical fibre to a Czerny-Turner monochromator (Jobin-Yvon Horiba) of 1 m focal length previously calibrated and equipped with a 2400 grooves/mm diffraction grating. A symphony CCD camera (CCD-1024×256-OPEN-STE) was used as radiation detector.

Nitrogen levels in the quartz reactor were monitored by using a quadrupole mass spectrometer (QMS, PTM63 112, mod. Omnistar, Pfeiffer Vacuum Technology) coupled to one of the lateral reactor outflows. A filter (Ref 33127-201 Iberfluid) was placed between the reactor and the spectrometer to prevent the entrance of solid carbon into the spectrometer.

The synthesized material was analysed by low-magnification TEM using a JEOL JEM 1400 operated at 120 kV and High-Resolution TEM (HRTEM) with a FEAI Tecnai G2F30 s-Twin microscope (0.2 nm point resolution) operated at 200 kV of accelerating voltage. Additionally, graphene samples supported in a glass substrate were characterized by Raman spectroscopy in the 750 – 3500 cm^{-1} using a Renishaw inVia confocal Raman Microscope equipped with a 514 nm and 20 mW NdYAG laser. XPS spectra were also obtained for attaining information about the graphene surface; for these purpose, a PHOIBOS 150 MCD with a double anode of Mg and Al was utilised. Finally, TGA analysis were carried out to evaluate the homogeneity, thermal stability and purity of the synthesized carbon material by using a Mettler Toledo TGA/DSC under aerobic conditions (50 mL/min) and a heating rate of 5 °C/min.

3. Results and discussion

3.1 Plasma external morphology and emitted spectra

A Casio Exilim EX-FH20 digital camera was used to take photographs of both pure Ar and Ar-EtOH plasmas. Figure 3a shows the torch generated with pure Ar for the experimental conditions of the current research (1 L/min flow and 300 W power). In this case, the plasma exposes a characteristic pinkish colour due to the entrance of N_2 coming from the surrounding air in the plasma. As an example, a spectrum of the Ar plasma torch operated at these conditions is presented in Figure 3b. This spectrum is mostly dominated by Ar atomic lines corresponding to transitions from 4p and 5p levels. However, not only Ar lines are detected, but also molecular bands associated to excited molecules and molecular ions of nitrogen (N_2 and N_2^+), respectively, and the other bands as CN, NO or CO. These species are formed by reactions between Ar atoms and ions with the N_2, O_2 and CO_2 contained in the air inside the reactor [37,47]. In pure Ar plasma, the presence of OH radical and the hydrogen atomic line H_α come from the decomposition of H_2O, which is present as impurity coming from the surrounded air.

Once the atmosphere is stable inside the reactor, the Ar-EtOH mixture was added to the plasma. Then, the discharge colour becomes green (Figure 3c) which is in line with the changes in the visible spectra emitted (Figure 3d). This colour change, due to the strong emission corresponding to C_2 species whose band-heads are in the 430 – 610 nm range of the spectrum (Figure 3d), proves that the ethanol molecules are being decomposed into the plasma. Besides, the drastic decrease of Ar emissions suggests that the energy supplied to the discharge is not being used only in the excitation/ionization of Ar atoms, but also in the dissociation/excitation of ethanol molecules [46]. The C_2 specie is considered as precursor of the graphene; thus, its presence in the Ar-EtOH plasma predicts the formation of graphene at the plasma exit. A couple of minutes after adding Ar-EtOH mixture to the discharge, a black powder is deposited on the reactor walls; then, the emission spectra must be taken before the appearance of this dark layer.

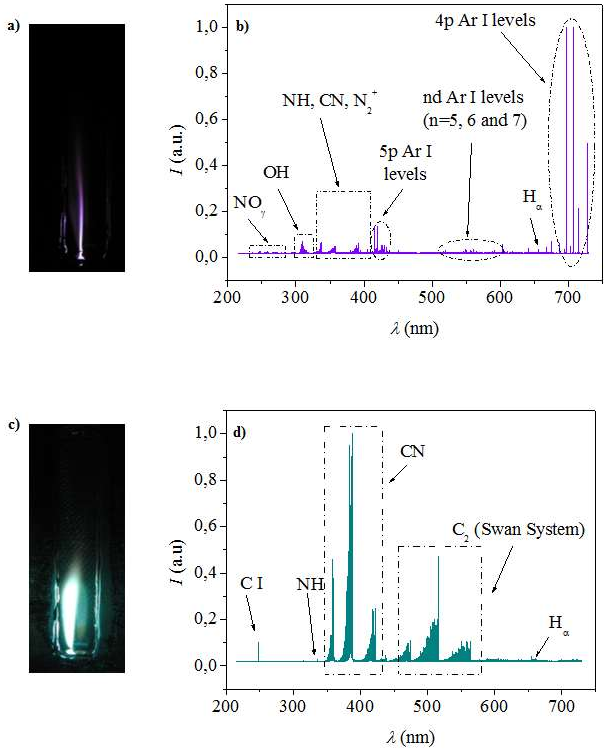

Figure 3. a) Pure Ar plasma, b) spectrum emitted by pure Ar plasma, c) Ar-EtOH plasma, d) spectrum emitted by Ar-EtOH plasma.

In [48], the formation of C_2 species from the decomposition of organic substances was also observed in Ar microwave discharges (in tubes) at low pressure. However, any nanostructured carbon material was reported. As it has been said before, in microwave plasmas the electrons are responsible for the gas heating taking the energy from the electromagnetic field and the elastic collisions between the electrons and the heavy particles. Plasmas generated at atmospheric pressure are collisional environments in which the electron density has a value $\geq 10^{14}$ cm^{-3}. This fact, favors these collisions and, consequently, the energy transference from electrons to heavy particles, increasing the gas temperature in comparison to low pressure plasmas. In particular, the introduction of ethanol in Ar TIAGO torch at atmospheric pressure gives place to an increase of the gas temperature from ≈ 3000 K (pure Ar) to ≈ 5000 K (Ar-EtOH) [41,46]; at low pressure, the gas temperature also raises with the entrance of ethanol into the discharge varying from an initial value of 1300 to 1900-2200 K [48]. In previous works [20,46], it was found that high temperature (≈ 3000 K) favors the formation of nanostructured carbon material. This fact explains why graphene is not obtained in microwave plasmas at low pressure. Then, we can say that two factors must be simultaneously present to induce the graphene formation: the formation of C_2 radicals and a high gas temperature

3.2 Graphene as product at the plasma exit

Graphene characterization

The black powder was scratched from the reactor and introduced into a vial (Figure 4). Low-magnification TEM images were obtained for different samples collected from the same vial (i.e. coming from the same extraction). For all these samples, the characteristic graphene structure is observed without the presence of any other nanostructured carbon material or carbonaceous particles. Besides, homogeneity in the structure can be also observed, identifying transparent zones which correspond to extended sheets, while darker zones correspond to folded graphene sheets.

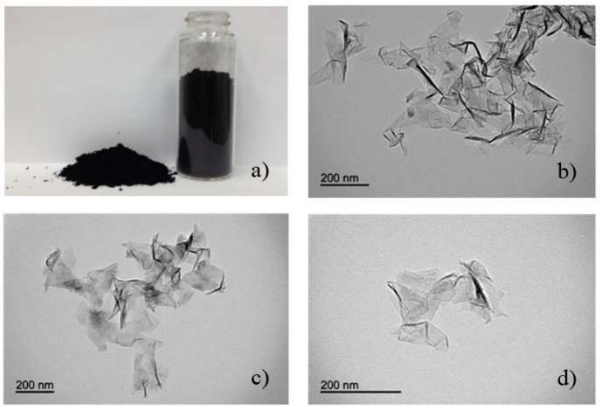

Figure 4. a) Synthesized graphene powder, b)-d) TEM images for samples taken from the graphene contained in the vial shown in a).

High-resolution TEM (HRTEM) images show that the produced graphene consists of few layer sheets without the presence of carbon nanotubes or graphitic particles (Figure 5). This indicates the selectivity of this procedure in the synthesis of pure graphene in relation to the formation of other carbon nanostructures

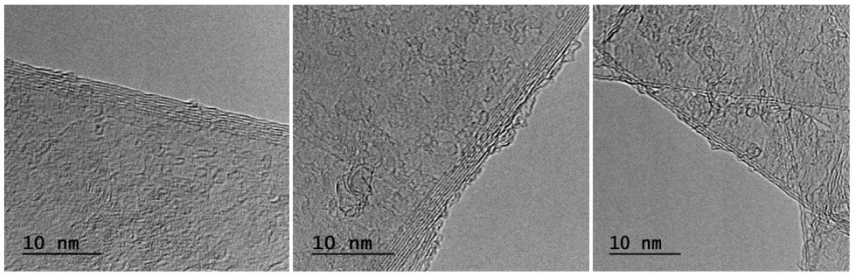

Figure 5. HRTEM images of the graphene shown in Figure 4.

A sample of the solid material was placed on a glass substrate to be analysed by Raman spectroscopy. Figure 6 shows a spectrum (750-3500 cm^{-1}) recorded with an acquisition

time of 30 s to avoid damages on the sample. The G and 2D bands characteristic of graphene [51] are present in the spectrum. The G band appearing at ~1580 cm^{-1} corresponds to the plane configuration of carbon atoms bonded with sp^2 hybridation; this location of G peak discards the presence of graphene oxide, which is slightly upshifted (~1594 cm^{-1}) [52,53]. The presence of the D band (~1352 cm^{-1}), first order zone boundary phonon mode, associated with defects in the graphene, presents a low intensity in comparison to the G band. Other bands as D' and G+D also assigned to defects in the graphene are observed but their intensity can be considered negligible in comparison to G and 2D bands [51]. The ratio I_D/I_G is habitually used to quantify the defects present in a graphene sample. For the graphene reported in Figure 6, the I_D/I_G value is 0.24, indicating a low number of defects. Similar ratios were found for all the analysed samples.

The I_D/I_G ratio can be also used to determinate the so-called the crystallite domain size (L_a) and the distance between defects (L_D) according to equations reported by Cançado and co-workers [54,55]. For our graphene, the L_a and L_D values derived from the Raman spectra are 69.6 and 22.4 nm, respectively, being similar values to graphene synthesized by CVD method [56-58].

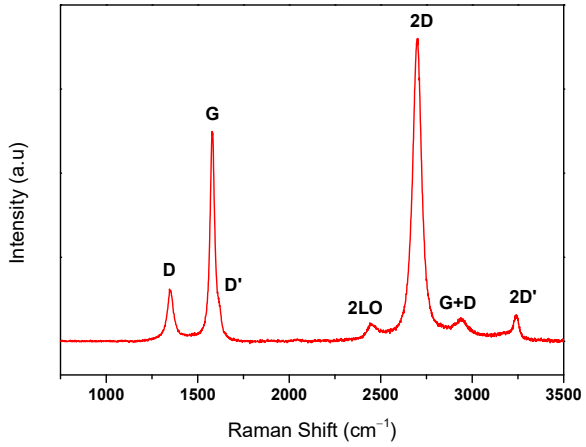

Figure 6. Raman spectrum of the synthesized graphene.

The 2D band is clearly visible in the spectrum and located at ~ 2700 cm^{-1} which is the region for few-layer graphene reported in the literature [56,59-65]. The line shape of the 2D peak, as well as its intensity relative to the G peak, can be used to characterize the number of layers [21,66-68]. Single-layer graphene is characterized by a very sharp, symmetric, Lorentzian 2D peak with intensity greater than twice the G peak. As the number of layers increases the ratio between the intensities of 2D and the G peaks tends to be lower than 2 and the 2D band becomes broader, less symmetric and its intensity decreases; thus, the 2D band in non-monolayer graphene can be resolved into two or more

components whereas monolayer graphene the 2D peak has a single component [68,69]. It is difficult to derive the number of graphene layers from the deconvolution of 2D peak; however, combining the results derived from the I_{2D}/I_G ratio (1.44) which is close to the value obtained by other authors [56,59-65,70,71],and HRTEM images it can be extracted that the graphene synthesized by our procedure consists of few layers (2-7 layers). In order to verify the reproducibility of the proposed graphene synthesis procedure, different batches (produced under the same experimental conditions) were analysed by Raman Spectroscopy, obtaining similar values for I_{2D}/I_G (> 1) and I_D/I_G (<< 1) ratios. These values appear depicted in Figure 7 and confirm the reproducibility of our synthesis method in terms of quality of the synthesized graphene.

Survey X-ray photoelectron spectroscopy (XPS) spectrum shows the presence of carbon atoms as majority element (98,5 At. %) (Figure 8a); and a small amount of oxygen that can be mainly attributed to the influence of the atmospheric oxygen during the extraction of graphene from the reactor. This agrees with the discussion about the location of G band in the analysis of the Raman spectrum . The deconvolution of C1s peak allowed us to carry out a detailed analysis of the types of carbons presents on the surface of the graphene (Figure 8b). The commercially available CasaXPS software was employed for this deconvolution. The C1s components were fitted using a Voigt function (70% Gaussian/ 30% Lorentzian). C1s core level XPS is mainly dominated by a peak at 284.4 eV which can be assigned to carbon with sp^2 hybridation. The deconvolution shows the presence of bands at 285.7, 286.2, 287.1 and 288.5 eV which, in agreement with previous reports [22,58,72-79], can be assigned to phenolic, epoxide, carbonyl and carboxyl groups, respectively. The low intensity found for the peak at 285.3 eV indicates the presence of low atomic percentage of carbons with sp^3 hybridation, which is associated to disorder or defects in graphene structures, confirming the results obtained from the analysis of Raman spectra (Figure 6). According to the literature, the high quality of the graphene synthesized in this work is corroborated by the presence of the shake-up satellite peak at 290.4 eV [57,59].

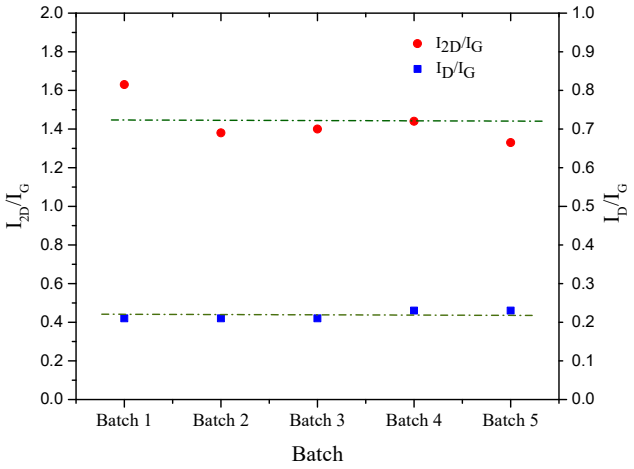

Figure 7. I_{2D}/I_G and I_D/I_G values for different sample batches under the same reaction conditions.

TGA analysis was also performed being Figure 9 a representative example of all the analysed samples. This figure shows both the TGA curve (line red) and derivative thermogravimetric curves (blue line) allowing the estimation of the temperature at which the sample experiences a loss of weight due to a combustion processes (in air environment). This temperature, commonly denominated oxidation temperature (T_o), calculated for our samples was around 550 ºC which is similar to the values reported in the literature for other graphene samples [79-82]. The presence of only one oxidation temperature at ≈ 550 °C, with a residual mass of almost 0 % is an additional evidence of the high purity of the graphene synthesized by the procedure herein presented. In addition, the absence of another T_o at 350-400 °C confirms that the analysed samples were free of amorphous carbon [73,83].

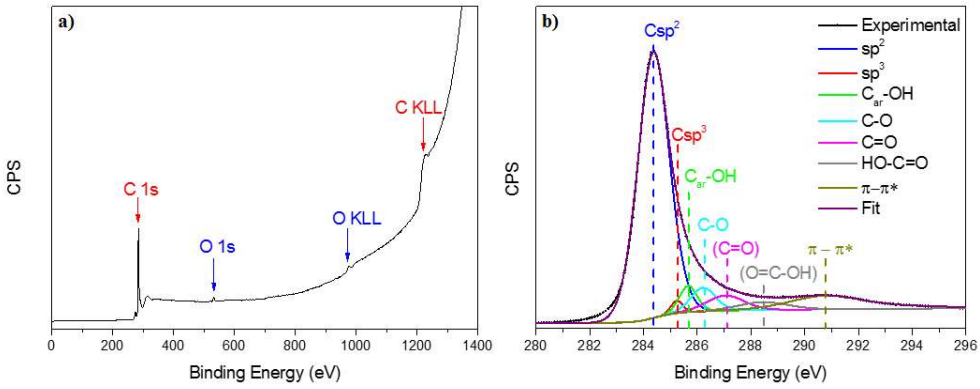

Figure 8. a) Survey XPS spectrum, b) C1s core level XPS spectrum.

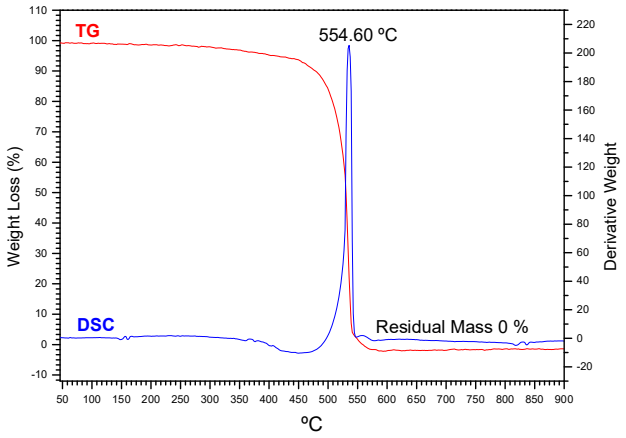

Figure 9. Thermogravimetric analysis in air of the synthesized graphene.

A comparison of the graphene synthesized by our procedure with one obtained by LPE was carried out. Raman analysis (Figure 10) and TEM images (Figure 11) are presented for both types of graphene. In figure 10, corresponding to the graphene obtained by TIAGO torch, the 2D band presents higher intensity, a more defined shape and much more less broadening, which is associated with a lower number of layers. As it has been mentioned before, the ratio between the intensities of 2D and G bands is a qualitative measure of the graphene quality. In this way, it can be observed that for graphene produced by TIAGO, the 2D peak intensity is higher than the G peak indicating that sheets are formed by only a few layers. Meanwhile, for the graphene produced by exfoliation, the D peak intensity is comparable to G peak and presents a significant broadening, which is a proof of the important number of defects in the material. The results of the Raman analyses agree with the TEM images (Figure 11). One observes that the transparency of graphene synthesized by our procedure is higher than for graphene obtained by graphite exfoliation. The darkened areas of the LPE graphene indicate that it is formed by much more layers than graphene produced from ethanol decomposition by TIAGO plasma torch.

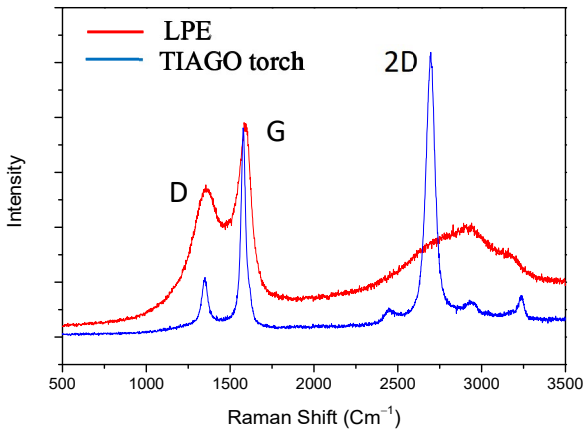

Figure 10. Raman spectra for graphene samples produced by LPE and TIAGO torch

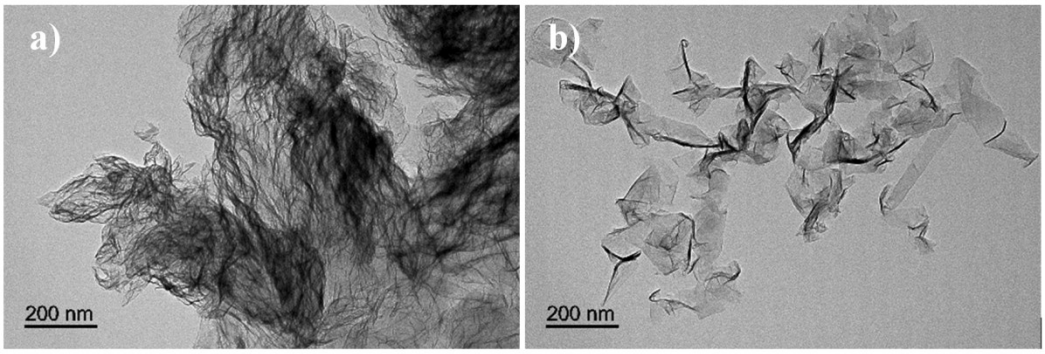

Figure 11. TEM images for graphene samples produced by a) LPE and b) TIAGO torch

4. Conclusions

In summary, we have presented a simple and effective method, based in microwave plasma technology, to produce graphene powder (2-7 layers) by using ethanol as carbon precursor. This technology solves one of the most important challenges facing the scientific community for graphene production, i.e., the synthesis of high-quality graphene in powder, catalyst-free and with the possibility to be scalable at industrial level. The production of graphene in powder has the advantage the possibility of obtaining solutions and dispersions by using different solvents depending of the intended application. The quality of the synthesized graphene is comparable to that obtained by using the traditional CVD technique or new developed procedures based on shear graphite exfoliation in liquids. The benefits of the use of the procedure reported here consist basically in four points:

a) the experimental setup can be connected in series of more than one device, which is not possible with the other experimental setups reported to date,

b) the use of a quartz reactor allows us to create the optimum environment to synthesize graphene,

c) the addition of ethanol in gas phase facilitates its decomposition and, therefore, less amount of ethanol is needed for obtaining graphene; unlike the systems adding the carbon precursor as aerosol (using Ar or bubbling Ar in ethanol) our system allows to feed the TIAGO device with known concentrations of a gaseous mixture,

d) metal catalysts are not needed to activate the growth processes, making this technique more environmentally friendly.

Finally, the use of ethanol as the carbon source contributes to the revalorization of waste for producing a high-value added product like graphene.

Acknowledgements

The authors of the present work are greatly thankful to Prof. Michel Moisan, head of the Groupe de Physique des Plasmas (University of Montreal), for the TIAGO torch donation within framework of our active collaboration. This research would not have been possible without this contribution. This research was partially supported by the Andalusia Regional Council from Spain (Consejería de Economía e Innovación) under the project no. P11-FQM-7489 (FEDER co-funded) and XXI Programa Propio de Fomento de la Investigación de la Universidad de Córdoba.

References

[1] J.C. Meyer, A.K. Geim, M.I. Katsnelson, K.S. Novoselov, T.J. Booth, S. Roth, The structure of suspended graphene sheets, Nature 446 (2007) 60

[2] H.Y. Wu, T. Yu, Z.X. Shen, Two-dimensional carbon nanostructures: fundamental, properties, synthesis, characterization, and potential applications, J. Appl. Phys 108 (2010) 071301

[3] Y. Yürüm, A. Taralp, T.N. Veziroglu, Storage of hydrogen in nanostructured carbon materials, Int. J. Hydrogen. Energy 34 (2009) 3784

[4] K. Ostrikov, U. Cvelbar, A.B. Murphy, Plasma nanoscience: setting directions, tackling grand challenges, J. Phys. D: Appl. Phys. 44 (2011) 174001

[5] A. Reina, X. Jia, J. Ho, D. Nezich, H. Son, V. Bulovic, M.S. Dresselhaus, J. King, Large area, few-layer graphene fimls on arbitrary substrates by chemical vapor deposition, Nano Lett. 9 (2009) 30

[6] W. Gannet, W. Regan, K. Watanabe, T. Taniguchi, M.F. Crommie, A. Zettl, Boron nitride substrates for high mobility chemical vapor deposited graphene, Appl. Phys. Lett. 98 (2011) 242105

[7] A. K. Geim, Graphene: Status and Prospects, Science 324 **(**2009) 1530–1534

[8] X. Lu, M. Yu, H. Huang, R. S. Ruoff, Tailoring graphite with the goal of achieving single sheets, Nanotechnology 10 **(**1999) 269

[9] T. Moldt, A. Eckmann, P. Klar, S. V. Morozov, A. A. Zhukov, K. S. Novoselov, C. Casiraghi, High-Yield Production and Transfer of Graphene Flakes Obtained by Anodic Bonding, ACS Nano 5 (2011) 7700–7706

[10] A. Shukla, R. Kumar, J. Mazher, A. Balan, Graphene made easy: High quality, large-area samples, Solid State Commun. 149 (2009) 718–721

[11] S. Dhar, A. R. Barman, G. X. Ni, X. Wang, X. F. Xu, Y. Zheng, S. Tripathy, A. Rusydi, K. P. Loh, M. Rubhausen, A. H. C. Neto, B. Őzyilmaz, T. Venkatesan, A new route to graphene layers by selective laser ablation, AIP Adv. 1 (2011) 22109

[12] D. A. Sokolov, K. R. Shepperd, T. M. Orlando, Formation of Graphene Features from Direct Laser-Induced Reduction of Graphite Oxide, J. Phys. Chem. Lett. 1 (2010) 2633–2636

[13] I. Vlassiouk, M. Regmi, P. Fulvio, S. Dai, P. Datskos, G. Eres, S. Smirno, Role of Hydrogen in Chemical Vapor Deposition Growth of Large Single-Crystal Graphene, ACS Nano 5 (2011) 6069–6076

[14] H. Zhang, Y. Zhan, B. Wang, Z. Chen, Y. Sui, Y. Zhang, T. Chumiao, B. Zhu, X. Xie, G. Yu, Z. Jin, X. Liu, Effect of Hydrogen in size-limited growth of graphene by atmospheric pressure chemical vapor, Journal of Elec Materi 44 (2015) 79-86

[15] X. Zhan, L. Wang, J. Xin, B. I. Yakobson, F. Ding, Role of hydrogen in graphene chemical vapor deposition growth on a copper surface, J. Am. Chem. Soc. 136 (2014) 3040-3047

[16] O. M. Maragó, F. Bonaccorso, R. Saija, G. Privitera, P. G. Gucciardi, M. A. Iatì, G. Calogero, P. H. Jones, F. Borghese, P. Denti, V. Nicolosi, A. C. Ferrari, Brownian Motion of Graphene, ACS Nano 4 (2010) 7515–7523

[17] J. Hassoun, F. Bonaccorso, M. Agostini, M. Angelucci, M. G. Betti, R. Cingolani, M. Gemmi, C. Mariani, S. Panero, V. Pellegrini, B. Scrosati, An Advanced Lithium-Ion Battery Based on a Graphene Anode and a Lithium Iron Phosphate Cathode, Nano Lett. 14 (2014) 4901–4906

[18] M. Lotya, Y. Hernandez, P. J. King, R. J. Smith, V. Nicolosi, L. S. Karlsson, F. M. Blighe, S. De, Z. Wang, I. T. McGovern, G. S. Duesberg, J. N. Coleman, Liquid Phase Production of Graphene by Exfoliation of Graphite in Surfactant/Water Solutions, J. Am. Chem. Soc. 131 (2009) 3611–3620

[19] K.R. Patonet et al. Scalable production of large quantities of defect-free few-layer graphene by shear exfoliation in liquids, nano Materials 13 (2014) 624-630

[20] R Rincón, C Melero, M Jiménez, M D Calzada, Synthesis of multi-layer graphene and multi-wall carbon nanotubes from direct decomposition of ethanol by microwave plasma without using metal catalysts, Plasma Sources Sci. Technol. 24 (2015) 32005

[21] A Dato, V Radmilovic, Z Lee, J Phillips, M Frenklach, Substrate-Free Gas-Phase Synthesis of Graphene Sheets, Nano Lett. 8 (2008) 2012–2016

[22] E. Tatarova, J. Henriques, C. C. Luhrs, A. Dias, J. Phillips, M. V. Abrashev, C. M. Ferreira, Microwave plasma based single step method for free standing graphene synthesis at atmospheric conditions, Appl. Phys. Lett. 103 (2013) 134101

[23] A. T. H. Chuang, B. O. Boskovic, J. Robertson, Freestanding carbon nanowalls by microwave plasma-enhanced chemical vapour deposition, Diam. Relat. Mater. 15 (2006) 1103–1106

[24] M. Meyyappan, L. Delzeit, A. Cassell, D. Hash, Carbon nanotube growth by PECVD: a review, Plasma Sources Sci. Technol. 12 (2003) 205

[25] Y. S. Kim, J. H. Lee, Y. D. Kim, S-K Jerng, K. Joo, E. Kim, J. Jung, E. Yoon, Y. D. Park, S. Seo, S-H Chun, Methane as an effective hydrogen source for single-layer graphene synthesis on Cu foil by plasma enhanced chemical vapor deposition, *Nanoscale* **5** (2013) 1221–1226

[26] M. Chhowalla, K. B. K. Teo, C. Ducati, N. L. Rupesinghe, G. A. J. Amaratunga, A. C. Ferrari, D. Roy, J. Robertson, W. I. Milne, Growth process conditions of vertically aligned carbon nanotubes using plasma enhanced chemical vapor deposition, J. Appl. Phys. 90 (2001) 5308

[27] S. Hofmann, B. Kleinsorge, C. Ducati, A. C. Ferrari, J. Robertson, Low-temperature plasma enhanced chemical vapour deposition of carbon nanotubes, Diam. Relat. Mater. 13 (2004) 1171–1176

[28] B. L. French, J. J. Wang, M. Y. Zhu, B. C. Holloway, Evolution of structure and morphology during plasma-enhanced chemical vapor deposition of carbon nanosheets, Thin Solid Films **494** (2006) 105–109

[29] J. Kim, M. Ishihara, Y. Koga, K. Tsugawa, M. Hasegawa, S. Iijima, Low-temperature synthesis of large-area graphene-based transparent conductive films using surface wave plasma chemical vapor deposition, Appl. Phys. Lett. 98 (2011) 91502

[30] T. Yamada, J. Kim, M. Ishihara, M. Hasegawa, Low-temperature graphene synthesis using microwave plasma CVD, J. Phys. D. Appl. Phys. 46 (2013) 63001

[31] M.D. Calzada, M.C. García, J.M. Luque, I. Santiago, Influence of the thermodynamic equilibrium state in the excitation of samples by a plasma at atmopsheric pressure, J. Appl. Phys. 92 (2002) 2269

[32] H-H. Kim, Current issues and future prospects, Plasma Process. Polym. 1 (2004) 91

[33] Y Kabouzi, M Moisan, J C Rostaing, C Trassy, D Guérin, D Kéroack, Z Zakrzewski, Abatement of perfluorinated compounds using microwave plasmas at atmospheric pressure, J. Appl. Phys. 93 (2003) 9483

[34] A. Dato, M. Frenklach, Substrate-free microwave synthesis of graphene: experimental conditions and hydrocarbon precursors, New J. Phys. 12 (2010) 125013

[35] E. Tatarova, A. Dias, J. Henriques, A. M. B. do Rego, A. M. Ferraria, M. V. Abrashev, C. C. Luhrs, J. Phillips, F. M. Dias, C. M. Ferreira, Microwave plasmas applied for the synthesis of free standing graphene sheets, J. Phys. D. Appl. Phys. 47 (2014) 385501

[36] M. Moisan, Z. Zakrzewski, J.C. Rostaing, Waveguide-based single and multiple nozzle plasma torches: the TIAGO concept, Plasma Sources Sci. T. 10 (2001) 387-394

[37] R. Rincón, J. Muñoz, M. Sáez, M. D. Calzada, Spectroscopic characterization of atmospheric pressure argon plasmas sustained with the Torche à Injection Axiale sur Guide d'Ondes, Spectrochim. Acta Part B At. Spectrosc. 81 (2013) 26–35

[38] R. Rincón, J. Muñoz, M. D. Calzada, Departure from Local Thermodynamic Equilibrium in argon plasmas sustained in a Torche à Injection Axiale sur Guide d'Ondes, Spectrochim. Acta Part B At. Spectrosc. 103–104 (2015) 14–23

[39] J. Marec, P. Leprince In: C.M. Ferrerira, M. Moisan, editors. 1993 Microwave discharges fundamentals and applications, Vol. 5, New York: Plenum

[40] C. I. M. Beenakker, A cavity for microwave-induced plasmas operated in helium and argon at atmospheric pressure, Spectrochim Acta B 31 (1976) 483-486

[41] R. Rincón, M. Jiménez, J. Muñoz, M. Sáez, M.D. Calzada, Hydrogen production from ethanol decomposition by two microwave tmopsheric pressure plsmas sources: surfatron and TIAGO torch, Plasma Chem. Plasma Process. 34 (2014) 145-147

[42] Y. Kabouzi, M. D. Calzada, M. Moisan, K. C. Tran, C. Trassy, Radial contraction of microwave-sustained plasma columns at atmospheric pressure, J. Appl. Phys 91 (2002) 1008-1019

[43] M. Jimenez, R. Rincón, A. Marinas, M.D. Calzada, Hydrogen production from ethanol decomposition by a microwave plasma: influence of the plasma gas flow, Int. J. Hydrogen Energy 38 (2013) 8708-8719

[44] N. Bundaleska, D. Tsyganov, R. Saavedra, E. Tatarova, F. M. Dias, C. M. Ferreira, Hydrogen production from methanol reforming in microwave "tornado"-type plasma, Int. J. Hydrogen Energy 38 **(**2013) 9145-9157

[45] D. Tsyganov, N. Bundaleska, E. Tatarova, C. M. Ferreira, Ethanol reforming into hydrogen-rich gas applying microwave "tornado"-type plasma, Int. J. Hydrogen Energy **38** (2013) 14512-14530

[46] R. Rincón, A. Marinas, J. Muñoz, M. D. Calzada, Hydrogen production from ethanol decomposition by microwave plasma TIAGO torch, Int. J. Hydrogen Energy 39 (2014) 11441–11453

[47] R. Rincón, A. Marinas, J. Muñoz, C. Melero, M. D. Calzada, Experimental research on ethanol-chemistry decomposition routes in a microwave plasma torch for hydrogen production, Chem. Eng. J. 284 (2016) 1117–26

[48] A. Yanguas-Gil, J. L. Hueso, J. Cotrino, A. Caballero, A. R. González-Elipe, Reforming of ethanol in a microwave surface-wave plasma discharge, Appl. Phys. Lett. 85 (2004) 4004

[49] J. Henriques, N. Bundaleska, E. Tatarova, F. M. Dias, C. M. Ferreira, Microwave plasma torches driven by surface wave applied for hydrogen production, Int. J. Hydrogen Energy 36 (2011) 345–54

[50] H. J. Boer, Liquid-Injection System Based on Mass Flow Controllers, Solid State Technology 39 (1996) 149-152

[51] I. Childres, L.A. Jauregui, W. Park, H. Cao, Y.P. Chen, Raman Spectroscopy of Graphene and related Matrials, Nova Science Publishers

[52] K. N. Kudin, B. Ozbas, H. C. Schniepp, R. K. Prud'homme, I. A. Aksay, R. Car, Raman Spectra of Graphite Oxide and Functionalized Graphene Sheets Nano Lett. 8 (2007) 36–41

[53] S. Stankovich, D. A. Dikin, R. D. Piner, K. A. Kohlhaas, A. Kleinhammes, Y. Jia, Y. Wu, S. T. Nguyen, R. Ruoff, Synthesis of graphene-based nanosheets via chemical reduction of exfoliated graphite oxide, Carbon N. Y. 45 (2007) 1558–1565

[54] L. G. Cançado, A. Jorio, E. H. M. Ferreira, F. Stavale, C. A. Achete, R. B. Capaz, M. V. O. Moutinho, A. Lombardo, T. S. Kulmala, A. C. Ferrari, Quantifying Defects in Graphene via Raman Spectroscopy at Different Excitation Energies, Nano Lett. 11 (2011) 3190–3196

[55] L. G. Cançado, K. Takai, T. Enoki, M. Endo, Y. A. Kim, H. Mizusaki, A. Jorio, L. N. Coelho, R. Magalhães-Paniago, M. A. Pimenta, General equation for the determination of the crystallite size la of nanographite by Raman spectroscopy, Appl. Phys. Lett. 88 (2006) 1–4

[56] A. Kumar, A. A. Voevodin, D. Zemlyanov, D. N. Zakharov, T. S. Fisher, Rapid synthesis of few-layer graphene over Cu foil, Carbon N. Y. 50 (2012) 1546–1553

[57] T. Terasawa, K. Saiki, Growth of graphene on Cu by plasma enhanced chemical vapor deposition, Carbon N. Y. 50 (2012) 869–74

[58] A. Guermoune, T. Chari, F. Popescu, S. S. Sabri, J. Guillemette, H. S. Skulason, T. Szkopek, M. Siaj, Chemical vapor deposition synthesis of graphene on copper with methanol, ethanol and propanol precursors, Carbon N. Y. 49 (2011) 4204–4210

[59] A. Malesevic, R. Vitchev, K. Schouteden, A. Volodin, L. Zhang, G. van Tendeloo, A. Vanhulsel, C. van Haesendonck, Synthesis of few-layer graphene via microwave plasma-enhanced chemical vapour deposition, Nanotechnology 19 (2008) 305604

[60] Z. Sun, Z. Yan, J. Yao, E. Beitler, Y. Zhu, J. M. Tour, Growth of graphene from solid carbon sources, Nature 468 (2010) 549–552

[61] J. Kim, S. B. Heo, G. H. Gu, J. S. Suh, Fabrication of graphene flakes composed of multi-layer graphene sheets using a thermal plasma jet system, Nanotechnology 21 (2010) 95601

[62] M. Passoni, V. Russo, D. Dellasega, F. Causa, F. Ghezzi, D. Wolverson, C. E. Bottani, Raman spectroscopy of nonstacked graphene flakes produced by plasma microjet deposition, J. Raman Spectrosc. 43 (2012) 884–888

[63] S. Lee, K. Lee, Z. Zhong, Wafer Scale Homogeneous Bilayer Graphene Films by Chemical Vapor Deposition, Nano Lett. 10 (2010) 4702–4707

[64] W. Liu, H. Li, C. Xu, Y. Khatami, K. Banerjee, Synthesis of high-quality monolayer and bilayer graphene on copper using chemical vapor deposition, Carbon N. Y. 49 (2011) 4122–4130

[65] M. P. Lavin-Lopez, J. L. Valverde, M. C. Cuevas, A. Garrido, L. Sanchez-Silva, P. Martinez, A. Romero-Izquierdo, Synthesis and characterization of graphene: influence of synthesis variables, Phys. Chem. Chem. Phys. 16 (2014) 2962–7290

[66] C. Casiraghi, S. Pisana, K. S. Novoselov, A. K. Geim, A. C. Ferrari, Raman fingerprint of charged impurities in graphene, Appl. Phys. Lett. 91 (2007) 233108

[67] A. C. Ferrari, Raman spectroscopy of graphene and graphite: Disorder, electron–phonon coupling, doping and nonadiabatic effects, Solid State Commun. 143 (2007) 47–57

[68] A. C. Ferrari, J. C. Meyer, V. Scardaci, C. Casiraghi, M. Lazzeri, F. Mauri, S. Piscanec, D. Jiang, K. S. Novoselov, S. Roth, A. K. Geim, Raman Spectrum of Graphene and Graphene Layers, Phys. Rev. Lett. 97 (2006) 187401

[69] D. Graf, F. Molitor, K. Ensslin, C. Stampfer, Spatially resolved Raman spectroscopy of single-and few-layer graphene, Nano Lett. **7** (2007) 238–242

[70] K. Masutani, T. Uchida, R. Irie, T. Katsuki, Catalytic asymmetric and chemoselective aerobic oxidation: kinetic resolution of *sec*-alcohols, Tetrahedron Lett. 41 (2000) 5119

[71] H. R. Aryal, S. Adhikari, H. Uchida, K. Wakita, M. Umeno, Few layers isolated graphene domains grown on copper foils by microwave surface wave plasma CVD using camphor as a precursor, 2D Mater. 3 (2016) 11009

[72] S. Yumitori, Correlation of C1s chemical state intensities with the O1s intensity in the XPS analysis of anodically oxidized glass-like carbon samples, J. Mater. Sci. 35 (2000) 139–146

[73] A. Ganguly, S. Sharma, P. Papakonstantinou, J. Hamilton, Probing the Thermal Deoxygenation of Graphene Oxide Using High-Resolution In Situ X-ray-Based Spectroscopies, J. Phys. Chem. C 115 (2011) 17009–17019

[74] J. Campos-Delgado, J. M. Romo-Herrera, X. Jia, D. A. Cullen, H. Muramatsu, Y. A. Kim, T. Hayashi, Z. Ren, D. J. Smith, Y. Okuno, T. Ohba, H. Kanoh, K. Kaneko, M. Endo, H. Terrones, M. S. Dresselhaus, M. Terrones, Bulk Production of a New Form of sp2 Carbon: Crystalline Graphene Nanoribbons, Nano Lett. 8 (2008) 2773–2778

[75] K. A. Wepasnick, B. A. Smith, J. L. Bitter, D. Howard Fairbrother, Chemical and structural characterization of carbon nanotube surfaces, Anal. Bioanal. Chem. **396** (2010) 1003–1014

[76] H. Liu, R. J. Hamers, An X-ray photoelectron spectroscopy study of the bonding of unsaturated organic molecules to the Si(001) surface, Surf. Sci. 416 (1998) 354–362

[77] M. J. Webb, P. Palmgren, P. Pal, O. Karis, H. Grennberg, A simple method to produce almost perfect graphene on highly oriented pyrolytic graphite, Carbon N. Y. 49 (2011) 3242–3249

[78] M. L. Bolen, R. Colby, E. A. Stach, M. A. Capano, Graphene formation on step-free 4H-SiC(0001), J. Appl. Phys. 110 (2011) 74307

[79] D. M. Crumpton, R. A. Laitinen, J. Smieja, D. A. Cleary, Thermal Analysis of Carbon Allotropes: An Experiment for Advanced Undergraduates, J. Chem. Educ. 6 (1996) 590-591

[80] V. Shanov, W. Cho, R. Malik, N. Alvarez, M. Haase, B. Ruff, N. Kienzle, T. Ochmann, D. Mast, M. Schulz, CVD growth, characterization and applications of carbon nanostructured materials, Surf. Coatings Technol. 230 (2013) 77–86

[81] W-W Liu, S-P Chai, A. R. Mohamed, U. Hashim, Synthesis and characterization of

graphene and carbon nanotubes: A review on the past and recent developments, J. Ind. Eng. Chem. 20 (2014) 1171–1185

[82] V. Chabot, B. Kim, B. Sloper, C. Tzoganakis, A. Yu, High yield production and purification of few layer graphene by Gum Arabic assisted physical sonication, Sci. Rep. 3 (2013)

[83] W-W Liu, A. Aziz, S-P Chai, A. R. Mohamed, C-T Tye, Preparation of iron oxide nanoparticles supported on magnesium oxide for producing high-quality single-walled carbon nanotubes, New Carbon Mater. 26 (2011) 255–261